PHYSICAL REVIEW D **79,** 116006 (2009)

Chiral symmetry restoration and deconfinement in Coulomb gauge QCD

Peng Guo and Adam P. Szczepaniak

Physics Department and Nuclear Theory Center Indiana University, Bloomington, Indiana 47405, USA

(Received 14 February 2009; published 16 June 2009)

In the framework of Coulomb gauge QCD we explore dynamical breaking of chiral symmetry and screening of the confinement potential at finite density. The screened potential is applied in the study of charmonium dissociation.

DOI: 10.1103/PhysRevD.79.116006 PACS numbers: 11.10.Ef, 12.38.Lg, 12.38.Mh, 12.40.−y

I. INTRODUCTION

Since the recent discovery of the strongly correlated QCD fluid, the phenomenology of the quark-gluon plasma has attracted a lot of attention [1]. Many predictions have been made for the several possible phases of the quark-gluon plasma in which quarks and gluons are no longer confined to nucleons and pions [2–5]. At extremely high temperature and low density, thermal excitations of the gluon field are expected to screen interactions between color charges and ultimately, due to asymptotic freedom result in a weakly interacting quark gas [6–8]. Similarly, at low temperature but high density Debye screening is expected to reduce the range of strong interactions. Novel phases that correlate quark color and flavor are predicted to occur at asymptotic densities due to the attractive nature of quark-quark interactions in certain color-flavor locked combinations [9,10]. Thus, finite temperature and/or density are expected to reflect on various aspects of confinement. Furthermore any modification of the ground state influences symmetry properties and, in particular, restoration of chiral symmetry is expected. At finite density and low temperature the precise relation between chiral symmetry restoration and deconfinement is not yet known. A common wisdom is that in this regime there is a phase transition from hadronic (confined) matter at low density to the unconfined (possibly superconducting) phase at higher densities [11–14]. Recently, however, it has been observed that the confined and deconfined phases may be separated by a phase where quarks are confined but chiral symmetry is restored. In the limit of an infinite number of colors $N_C \to \infty$ this so-called quarkyonic phase would in fact extend to infinite density, since in this limit Debye screening due to quark loop vanishes [15]. In this paper we examine the possible emergence of this new phase using a canonical formulation of the QCD many body problem in the Coulomb gauge. The Coulomb gauge canonical formulation can describe both finite temperature and density. In this formulation manifestation of deconfinement can be inferred from the temperature and/or density dependence of the color Coulomb interaction. In contrast, lattice simulations at finite density are still at their infancy [16,17]. One of the smoking gun signals of deconfinement is the possible dissociation of heavy quarkonia [18–25]. By studying the density dependence of the Coulomb gauge heavy quark potential we will be able to explore charmonium properties at finite density.

The paper is organized at follows: In the following section we discuss the Coulomb gauge QCD and approximations relevant to the problem in hand. Zero and finite density properties are discussed in Secs. III and IV, respectively. Charmonium dissociation is studied in Sec. V and followed by conclusions and outlook.

II. COULOMB GAUGE QCD

In this section we briefly discuss QCD in the Coulomb gauge and the approximations appropriate for the high density and/or temperature systems [26,27]. In the Coulomb gauge gluons are described by the transverse potentials $\mathbf{A}^a(\mathbf{x})$, $a = 1 \cdots N_C^2 - 1$, $\boldsymbol{\nabla} \cdot \mathbf{A}^a(\mathbf{x}) = 0$ and the conjugated, transverse momenta $\boldsymbol{\Pi}^a(\mathbf{x})$,

$$[\mathbf{A}^a(x), \boldsymbol{\Pi}^b(\mathbf{y})] = i\boldsymbol{\delta}_T(\mathbf{x} - \mathbf{y})\delta^{ab}, \tag{1}$$

where $\boldsymbol{\delta}_T(\mathbf{x} - \mathbf{y}) \equiv [\mathbf{I} - \boldsymbol{\nabla}\boldsymbol{\nabla}/\boldsymbol{\nabla}^2]\delta^3(\mathbf{x} - \mathbf{y})$. The canonical momentum $\boldsymbol{\Pi}^a(\mathbf{x})$ is the negative of the transverse component of the chromo-electric field. The quark and antiquark degrees of freedom will be defined below in terms of the canonical set of Dirac fields $\psi_i(\mathbf{x})$, $\psi_i^\dagger(\mathbf{x})$, $i = 1 \cdots N_C$, one for each flavor. The Hamiltonian is given by

$$H = H_D + H_{\mathrm{YM}} + H_C, \tag{2}$$

where H_D contains the Dirac kinetic energy and quark-transverse gluon interaction, H_{YM} is the Yang-Mills term, which contains the gluon kinetic energy and the three- and four-gluon interactions and finally H_C is the Coulomb potential given by

$$H_C = \frac{1}{2}\int d\mathbf{x}d\mathbf{y}\mathcal{J}^{-1}\rho^a(\mathbf{x})K(\mathbf{x}, a; \mathbf{y}, b)[\mathbf{A}]\mathcal{J}\rho^b(\mathbf{y}). \tag{3}$$

It represents the non-Abelian Coulomb gauge interaction between color charge densities $\rho^a(\mathbf{x}) = \psi^\dagger(\mathbf{x})T^a\psi(\mathbf{x}) + f_{abc}\mathbf{A}^b(\mathbf{x})\boldsymbol{\Pi}^c(\mathbf{x})$ mediated by the Coulomb kernel $K[\mathbf{A}]$ given by

$$K(\mathbf{x}, a; \mathbf{y}, b)[\mathbf{A}] = \left[\frac{g}{\boldsymbol{\nabla}\cdot\mathcal{D}}(-\boldsymbol{\nabla}^2)\frac{g}{\boldsymbol{\nabla}\cdot\mathcal{D}}\right]_{(\mathbf{x},a;\mathbf{y},b)}. \tag{4}$$

Finally, $\mathcal{J} = \det[-\nabla\cdot\mathcal{D}]$ is the determinant of the

Faddeev-Popov operator; $\mathcal{D} = \mathcal{D}_{ab} = \delta_{ab}\boldsymbol{\nabla} + g f_{acb}\mathbf{A}^c$ is the covariant derivative in the adjoint representation, and $\mathbf{B}$ is the chromo-magnetic field $\mathbf{B}^a(\mathbf{x}) = \boldsymbol{\nabla} \times \mathbf{A}^a(\mathbf{x}) + (g/2) f_{abc}\mathbf{A}^b(\mathbf{x}) \times \mathbf{A}^c(\mathbf{x})$. At every space point $\mathbf{x}$ and color component a the Coulomb gauge potentials, $\mathbf{A}^a(\mathbf{x})$ are an analog of a curvilinear coordinate. This is because their values are restricted to reside within the boundary of the Gribov region, which has a nontrivial metric determined by $\mathcal{J}$ [28]. A confinement scenario in the Coulomb gauge states that it is the field configurations near the boundary of the Gribov region $\partial\Omega$ that dominate the QCD vacuum [29,30], and it follows that fluctuations near the boundary lead to massive quasiparticle excitations. Since the exact parametrization of the Gribov horizon is not known the quantitative description of this confinement scenario varies depending on how restriction to the Gribov horizon is implemented, but the general features seem to be robust [31–34]. With this picture in mind we approximate the ground state of a finite density quark plasma by the state with no quasiparticle gluon excitations, and the large background fields concentrated near $\partial\Omega$ lead to enhancement in the long-range behavior of the Coulomb kernel [26,34]. That is we make the replacement

$$K(\mathbf{x}, a; \mathbf{y}, b)[\mathbf{A}] \rightarrow \langle K(\mathbf{x}, a; \mathbf{y}, b)[\mathbf{A}]\rangle = K(\mathbf{x} - \mathbf{y})\delta_{ab}, \tag{5}$$

with the potential $K(r)$ modified from its free ($\mathbf{A} = 0$) form $K(r) = \alpha/r$, for large r due to the large fields $\mathbf{A} \in \partial\Omega$. In particular, we approximate the kernel by the from

$$K(r) = K_C(r) + K_L(r), \tag{6}$$

with K_C and K_L being the short-range Coulomb and long-range linear potentials, respectively, which will be discussed in detail in the following section. The final Hamiltonian, describing massless quarks with energies below gluon quasiparticle excitations is given by

$$H = \int d\mathbf{x}\,\psi^\dagger(x)(-i\boldsymbol{\alpha}\cdot\boldsymbol{\nabla})\psi(x) + \frac{1}{2} \times \int d\mathbf{x}d\mathbf{y}\,\psi^\dagger(x)T^a\psi(x)K(|\mathbf{x}-\mathbf{y}|)\psi^\dagger(y)T^a\psi(y). \tag{7}$$

Note, that from Eq. (7) it follows that it is $-C_F K(r)$, which is the instantaneous interaction in the color-singlet $q\bar{q}$ channel.

III. QUARKS AT ZERO DENSITY

In presence of the effective density-density interaction mediated by the kernel K, in Eq. (7) quarks and antiquarks acquire effective mass, which in the mean field approximation can be described within the Hartree-Fock-Bogolubov framework [11–13,35]. The single quark quasiparticle operators are defined by a canonical transformation to a plane wave representation of the Dirac fields.

$$\psi(\mathbf{x}) = \sum_\lambda \int d\mathbf{k}\, e^{i\mathbf{k}\cdot\mathbf{x}}[u(\mathbf{k},\lambda)b_{\mathbf{k},\lambda} + v(-\mathbf{k},\lambda)d^\dagger_{\mathbf{k},\lambda}] \tag{8}$$

and similarly for $\psi^\dagger$. Here, $d\mathbf{k} \equiv d^3k/(2\pi)^3$, $\lambda = \pm 1/2$ is the quark (antiquark) spin projection and $b(d)$, $b^\dagger(d^\dagger)$ are the quark (antiquark) annihilation and creation operators, respectively. These quasiparticle operators satisfy the standard fermion anticommutation relations and define the vacuum state by $b_{\lambda,\mathbf{k}}|\text{vac}\rangle = d_{\lambda,\mathbf{k}}|\text{vac}\rangle = 0$. The single particle wave functions are given by

$$\begin{aligned} u^T(\lambda,\mathbf{k}) &= \frac{1}{\sqrt{2}}\left(\sqrt{1+\frac{E_k}{m_k}}\chi_\beta, \sqrt{1-\frac{E_k}{m_k}}\sigma\cdot\hat{\mathbf{k}}\chi_\beta\right) \\ v^T(\lambda,\mathbf{k}) &= \frac{1}{\sqrt{2}}\left(\sqrt{1-\frac{E_k}{m_k}}\sigma\cdot\hat{\mathbf{k}}\bar{\chi}_\beta, \sqrt{1+\frac{E_k}{m_k}}\bar{\chi}_\beta\right), \end{aligned} \tag{9}$$

where $\bar{\chi} \equiv i\sigma_2\chi$, $m_k/E_k \equiv \sin\phi_k$ and ϕ_k is the BCS angle, which determines the number density of quark-antiquark pairs in the BCS vacuum, i.e. the quark condensate and the extent of chiral symmetry breaking [36–38]. At zero temperature and density the BCS angle is determined by minimizing the vacuum energy density $\delta\langle\text{vac}|H|\text{vac}\rangle/\delta\phi_k = 0$, which leads to the gap equation ($s_p \equiv \sin\phi_p$, $c_p \equiv \cos\phi_p$)

$$p s_p = \frac{C_F}{2}\int d\mathbf{k}\,\tilde{K}(|\mathbf{k}-\mathbf{p}|)[s_k c_p - c_k s_p \hat{\mathbf{k}}\cdot\hat{\mathbf{p}}]. \tag{10}$$

Here, $\tilde{K}(p)$ is the Fourier transform of the effective potential from Eq. (4). The Fourier transform of the linear potential K_L has to be taken with care, since naively, $\int d\mathbf{x}|x|\exp(-\mathbf{k}\cdot\mathbf{x}) = \infty$. We introduce an infrared regulator ϵ and define [39]

$$K_L(r) \rightarrow K_{L,\epsilon}(r) = \frac{2b}{\epsilon^2}\left(\frac{1}{R} - \frac{e^{-\epsilon R}}{R}\right) - \frac{2b}{\epsilon} \tag{11}$$

so that $\lim_{\epsilon\rightarrow 0} K_{L,\epsilon}(r) = -br$. The difference between the linear potential and the IR finite approximation is shown in Fig. 1. In momentum space the IR finite kernel becomes

$$\tilde{K}_{L,\epsilon}(p) = \frac{8\pi b}{p^2(p^2+\epsilon^2)} - \frac{2b}{\epsilon}(2\pi)^3\delta^3(\mathbf{p}). \tag{12}$$

It is clear that the δ term does not contribute the gap Eq. (10) and the gap equation is well defined in the limit $\epsilon \rightarrow 0$. Equivalently, the gap equation is invariant under a constant shift in the potential

$$K(r) \rightarrow K(r) + C. \tag{13}$$

Since such a shift induces a contribution to the Hamiltonian proportional to the square of the total charge operator $\sum_a Q^a Q^a$,

$$Q^a = \int d\mathbf{x}\rho^a(\mathbf{x}) \tag{14}$$

invariance under (13) is an exclusive property of color-singlet states, and it is only matrix element invariant under

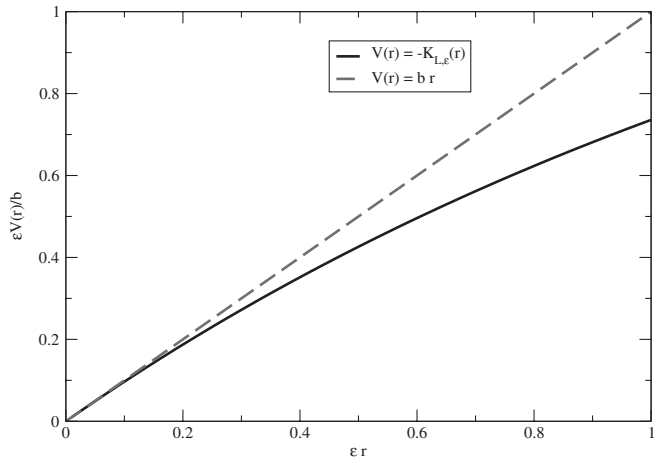

FIG. 1. IR finite approximation to the linear potential of Eq. (11). The proper potential for describing the color-nonsinglet state, [cf. Eq. (11)] corresponds to a downward shift by two units.

global color rotations that are physical. In contrast, under this shift, the energy Ω_p of a single quark state $(b^\dagger(\lambda, \mathbf{p})|\text{vac}\rangle)$ that is given by

$$\Omega_p = pc_p + \frac{C_F}{2}\int d\mathbf{k}\tilde{K}(|\mathbf{k}-\mathbf{p}|)[s_k s_p + c_k c_p \hat{\mathbf{k}}\cdot\hat{\mathbf{p}}] \tag{15}$$

transforms to

$$\Omega_p \to \Omega_p + \frac{C_F}{2}C. \tag{16}$$

So single quark states are clearly unphysical. For $\epsilon \to 0$ the δ term in $\tilde{K}$ dominates the integrand in Eq. (15), and the quark self-energy becomes negative and tends to $-\infty$ in the $\epsilon \to 0$ limit. As pointed out in [39] this is necessary in order for color-singlet $q\bar{q}$ excitations to have finite, non-negative energies. This is because the potential energy in the $q\bar{q}$ bound state, given by $-C_F\tilde{K}(p)$, where p is the relative momentum between the quark and the antiquark is large and positive for small ϵ (and approached $+\infty$ in the limit $\epsilon \to 0$). Thus, the infinities in the $\epsilon \to 0$ limit cancel between the self-energies and the residual interaction between the quark and the antiquark. Since $\phi \neq 0$ is a lower energy state compared to $\phi = 0$, after cancellation of the IR divergencies, the finite energy of color single excitations is C independent and non-negative. This is, however not the case for color-nonsinglet states. For example, a single quark state with energy given by Eq. (15) has negative energy, which becomes $-\infty$ in the limit when the interaction is confining (i.e. $\epsilon \to 0$). This is clearly unphysical as one would expect colored states to have positive, and IR diverging energies, $\Omega \to +\infty$ in the confining limit. Since the shift in Eq. (13) is a symmetry of the physical sector we can choose C to cancel the IR divergence in the quark self-energy, and redefine K_L accordingly Thus, instead of Eq. (12) we should use

$$\tilde{K}_{L,\epsilon}(p) = \frac{8\pi b}{p^2(p^2+\epsilon^2)}, \tag{17}$$

which is positive, gives $\Omega \to +\infty$ as $\epsilon \to 0$ and does not affect properties of color-singlet states. In fact, an interaction without the IR divergent constant term constant term is obtained when computing the expectation value of $K[A]$ [cf. Eq. (4)] in a mean field ansatz for the gluon vacuum distribution [26,27].

A similar argument for regulating the $\mathbf{p} = 0$ singularity of $\tilde{K}_L$ was proposed in [40]. There by explicitly restricting the spectrum of the Hamiltonian to include only the color-singlet subspace an even stronger constraint on the IR momentum dependence of the kernel was derived, namely, $\tilde{K}_L(0) = 0$. With an IR regulated (finite-ϵ) kernel the minimal physical requirement, however is that colored excitations have positive energies, (becoming $+\infty$ as $\epsilon \to 0$). Thus, we do consider kernels $\tilde{K}(p)$ that have integrable, but in principle finite zero modes.

IV. QUARKS AT FINITE DENSITY

With the interactions in the Hamiltonian now well defined in the IR, the system at finite quark density can be described using standard many body techniques [11–13]. In particular, the finite density gap equation becomes

$$ps_p = \frac{C_F}{2}\int d\mathbf{k}(1-n_k)\tilde{K}_{\text{eff}}(|\mathbf{k}-\mathbf{p}|)[s_k c_p - c_k s_p \hat{\mathbf{k}}\cdot\hat{\mathbf{p}}], \tag{18}$$

and the single quark energy is given by

$$\Omega_p = pc_p + \frac{C_F}{2}\int d\mathbf{k}(1-n_k)\tilde{K}_{\text{eff}}(|\mathbf{k}-\mathbf{p}|) \times [s_k s_p + c_k c_p \hat{\mathbf{k}}\cdot\hat{\mathbf{p}}]. \tag{19}$$

Here, n_k is the quark occupation number at zero temperature,

$$n_k = \theta(k_F - k), \tag{20}$$

with k_F denoting the Fermi momentum. Because of the Pauli blocking factor $1 - n_k$ interactions between quarks have small effect on quark levels inside the Fermi sphere where quarks are effectively free $\Omega_p \sim pc_p$. The self-energy contributes mainly for states above the Fermi surface and results in states that are similar to the confined quark states at zero density. Since any modification of the antiquark distribution from its vacuum value is suppressed at finite quark density, we have set the antiquark occupation number to be zero, and in the following we only consider quark-hole excitations near the quark Fermi surface. We use the Fermi momentum to count the quark states because at zero temperature it is directly related to quark density. Furthermore, due to the attractive, long-range interaction the single quark energies are large, even

for a screened potential and the same is true for the chemical potential; it takes large energy to remove a quark. So, instead of treating Fermi momentum as a function of the large single quark energy and chemical potential, we treat Fermi energy as a function of the Fermi momentum. For small Fermi momentum, i.e. low density, screening is weak and the energy to remove a single quark tends to infinity.

A. Screening effect at finite density

At finite density the quark-quark potential $C_F\tilde{K}(p)$ is screened by particle-hole excitations near the Fermi surface, resulting in the effective interaction $C_F\tilde{K}_{\rm eff}(p)$, which enters Eqs. (18) and (19),

$$\begin{aligned}\tilde{K}_{\rm eff}(p) &= \tilde{K}(q) - \tilde{K}(q)\Pi(q)\tilde{K}(q) + \cdots \\ &= \tilde{K}(q) - \tilde{K}(q)\Pi(q)\tilde{K}_{\rm eff}(q),\end{aligned} \tag{21}$$

or

$$\tilde{K}_{\rm eff}(q) = \frac{\tilde{K}(q)}{1 + \tilde{K}(q)\Pi(q)}. \tag{22}$$

The vacuum polarization, $\Pi(q)$ is shown in Fig. 2, and it describes the probability for creating a particle-hole excitation. Since the pair is excited in the colored state in the confining limit ($\epsilon \to 0$) it is expected that $\Pi(q) \to 0$, since the amplitude is proportional the inverse of the particle-hole excitation energy, which becomes infinite in the confining limit. Assuming phase transition does take place, however, we can examine the effect of Debye screening in the deconfined phase near or above the phase transition density. In this case vacuum polarization is given by

$$\begin{aligned}\Pi(q) = -\frac{n_f}{2}\int d\mathbf{k}\,\frac{n_k - n_{|\mathbf{k}+\mathbf{q}|}}{\Omega_k - \Omega_{|\mathbf{k}+\mathbf{q}|}} \times \Big[1 + s_k s_{|\mathbf{k}+\mathbf{q}|} \\ + c_k c_{|\mathbf{k}+\mathbf{q}|}\frac{\mathbf{k}\cdot(\mathbf{k}+\mathbf{q})}{k(|\mathbf{k}+\mathbf{q}|)}\Big],\end{aligned} \tag{23}$$

where n_f is the number of light flavors. The set of equations (18), (19), (22), and (23) with $\tilde{K}(p)$ given by

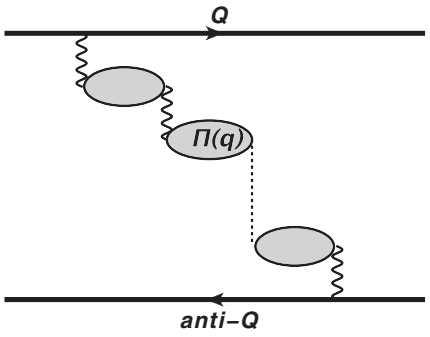

FIG. 2. Vacuum polarization Π_q.

$$\tilde{K}(p) = \frac{4\pi\alpha(p)}{p^2} + \frac{8\pi b}{p^2(p^2+\epsilon^2)} \tag{24}$$

forms a set of coupled equations, which we solve numerically and discuss below.

B. Numerical result

We solved coupled Eqs. (18), (19), (22), and (23) at finite density and zero temperature with two light quarks flavors using

$$\alpha(p) = \frac{4\pi Z}{\beta^{3/2}\log^{3/2}(\frac{p^2}{\Lambda_{\rm QCD}^2} + c)}, \tag{25}$$

with $Z = 5.94$, $c = 40.68$, and $\Lambda_{\rm QCD} = 250$ MeV determined from fitting the zero-density $q\bar{q}$ potential [41]. At zero density what makes quark energies finite is the IR regulator ϵ in Eq. (24), at finite density, above the deconfinement phase transition we expect, however, that the self-consistent set of equations will admit nontrivial solutions in the limit $\epsilon \to 0$, with the Fermi momentum k_F taking over the role of the IR regulator instead. We have verified numerically that this indeed is the case. The equations are solved by iterations. For given density, k_F we start with a small, but finite ϵ, e.g. $\epsilon = 0.008$ GeV, so the self-energy at the first iteration has a sharp jump at the Fermi surface (see left panel in Fig. 5). At this initial state the vacuum polarization is highly suppressed (see left panel in Fig. 6), particularly for small momenta. After a few iterations, however, the self-energy becomes regulated by the vacuum polarization itself and simultaneously the vacuum polarization increases at small momenta. Finally, we reduce the initial value of the IR regulator ϵ, and we verify that after several iterations solutions converge to the same value, regardless of the starting value of the regulator. We repeat the calculations for several values of the Fermi energy. We show these final results for the effective potential, BCS gap angle, quark single energy, and vacuum polarization in Figs. 3–6, respectively.

It is often stated that chiral symmetry restoration and deconfinement occur simultaneously [11,12]. Our calculation illustrates that this need not be the case. At finite density, effective potential is already deconfined, but the gap equation admits nontrivial solutions. Only when the Fermi momentum increases above, approximately $k_F \sim$ 0.05 to 0.06 GeV, the effective potential at large distance is not strong enough to sustain spontaneous chiral symmetry breaking.

C. Quarkyonic matter

Another manifestation of the independence of chiral symmetry restoration and deconfinement is the appearance of confined, chirally symmetric, quarkyonic, matter [15]. Since $K \propto g^2 \propto 1/N_C$ we can extract explicit N_C dependence of the effective interaction

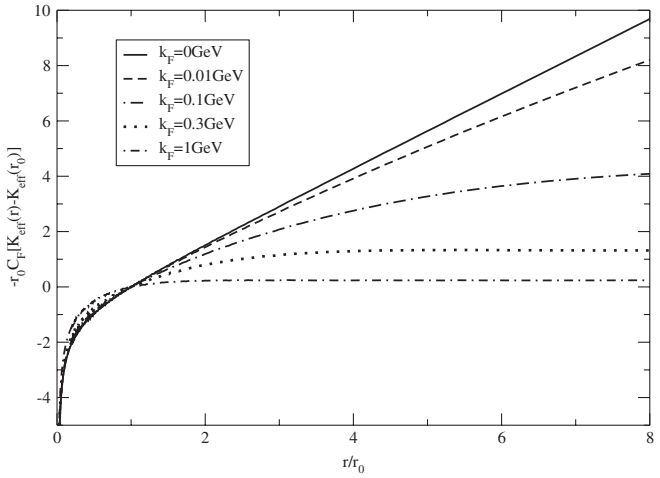

FIG. 3. Effective potential at finite density ($r_0 = 1/0.45\ \mathrm{GeV}^{-1}$).

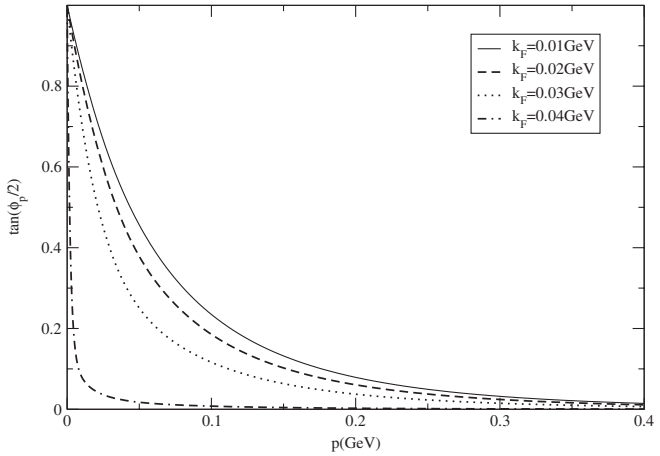

FIG. 4. Solution of gap equation ϕ_k at finite density. For $k_F \gtrsim 0.05$ GeV the solution of the gap equation is $\phi(p) = 0$.

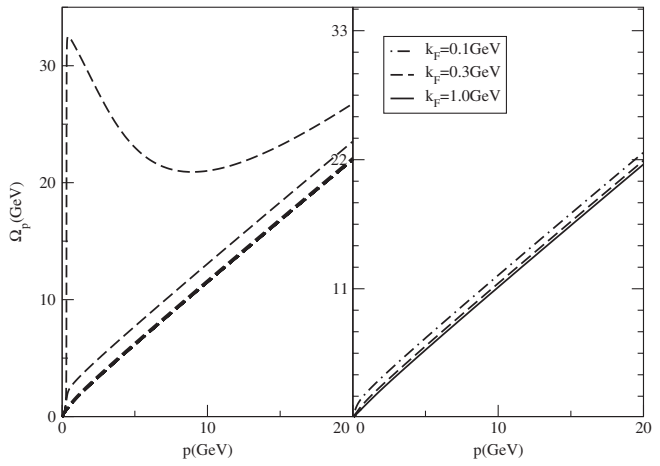

FIG. 5. Left panel: Variation of single quark energy Ω_p through iterations for $k_F = 0.3$ GeV. Ω_p is the largest at first iteration. Right panel: Ω_p at the end of the iterations.

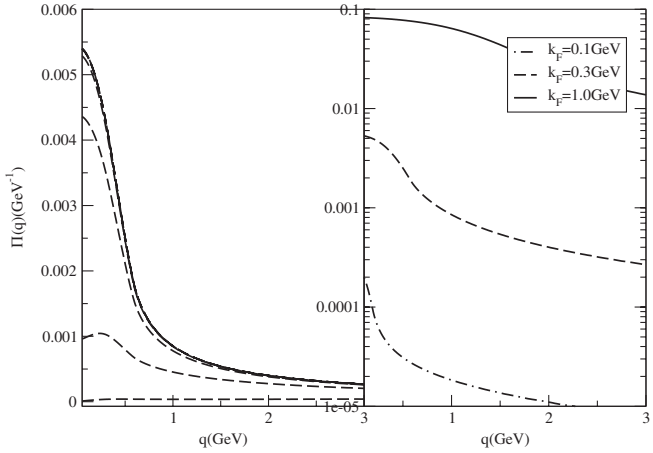

FIG. 6. Same as in Fig. 5 for vacuum polarization Π_q. In the left panel, $\Pi(q)$ is the smallest at first iteration.

$$\tilde{K}^{N_C}_{\mathrm{eff}} = \frac{\frac{3}{N_C}\tilde{K}^{N_C=3}}{1+\frac{3}{N_C}\tilde{K}^{N_C=3}\Pi}. \tag{26}$$

The $q\bar{q}$ potential being proportional to $C_F K^{N_C}_{\mathrm{eff}}$ at large N_C becomes

$$C_F K_{\mathrm{eff}} \to \tfrac{3}{2}\tilde{K}^{N_C=3}, \tag{27}$$

since the vacuum polarization contribution is suppressed in the $N_C \to \infty$ limit. In this limit we thus find that the Debye screening disappears and confinement is restored at any density. The gap Eq. (18), however is not affected by the large N_C limit, and the Pauli blocking remains in effect. Thus, as density increases it will eventually prevent the gap equation from developing a nontrivial, chirally broken solution [14].

V. CHARMONIUM BINDING AT FINITE DENSITY

Modifications of charmonium properties, in particular, binding energy and size may be strongly affected when the bound state propagates through the plasma. At finite temperature such modifications have been studied by computing charmonium spectrum using a temperature-dependent static potential that is extracted from the lattice calculation [18–20]. With such temperature-dependent static potential, melting of charmonium can be inferred from the temperature dependence of the spectral function [24,25] or by directly solving the bound state Shrödinger equation [22,42]. In the former approach, melting of charmonium can be seen when the bound state peak of spectral function collapses, and as temperature increases it becomes buried under the continuous background. From Shrödinger equation calculation melting is inferred at a temperature when the bound state solution disappears. The melting temperature of the J/Ψ from these two different approaches appears to be in a very good agreement at approximately $1.6T_c$. Here, we use the Shrödinger equation approach to

TABLE I. J/Ψ and Ψ' energy spectrum at finite density.

k_F (GeV)	J/Ψ (GeV)	Ψ' (GeV)	$\langle r\rangle_{J/\Psi}$ (GeV^{-1})
0.0	3.065	3.823	1/0.476
0.2	2.801	3.288	1/0.417
0.4	2.771	2.946	1/0.351
0.6	2.733	2.771	1/0.250
0.8	2.682	2.683	1/0.050

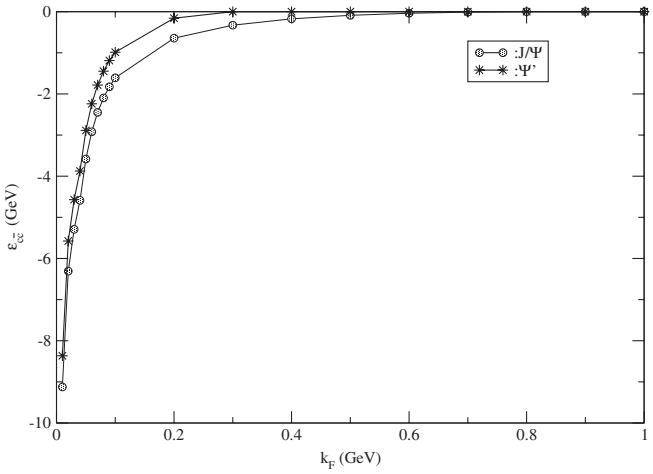

FIG. 7. $\epsilon_{J/\Psi}$ and $\epsilon_{\Psi'}$ at finite density, where $\epsilon_{J^{PC}}$ is defined in Eq. (29).

calculate dissociation of the J/Ψ at finite density with two flavors of light quarks. The mass $M_{J^{PC}}$ of the J/Ψ is given by

$$M_{J^{PC}} = \epsilon_{J^{PC}} + 2m + C_F[K_{\text{eff}}(r_0) - K_{CL}(r_0)], \qquad (28)$$

and

$$\left(\epsilon_{J^{PC}} - \frac{q^2}{m}\right)\Psi^N_\alpha(q) = -C_F\sum_{\alpha'}\int d\mathbf{q}' P_{L'_q}(\hat{\mathbf{q}}\cdot\hat{\mathbf{q}}') \times \tilde{K}_{\text{eff}}(|\mathbf{q}-\mathbf{q}'|)\Psi^N_{\alpha'}(q'), \qquad (29)$$

with N being the radial quantum number, $\alpha = (S_q, L_q)$ stands for total quark spin S_q and relative orbital angular momentum L_q. The heavy (charm) quark mass, m absorbs any finite shift that has been removed from K_{eff} as discussed in Sec. III and is fixed, by fitting spin-averaged $L_q = 0$ charmonium masses $\bar{M}^S_{c\bar{c}} = \frac{1}{4}[M_{0^{-+}} + 3M_{1^{--}}] = 3.068$ GeV. The energy of J/Ψ and its first radial excitation as a function of the light quark density are given in Table I, and the binding energy is plotted in Fig. 7. From our numerical evaluation it follows that melting occurs at light quark density $k_F \sim 0.9$ GeV for J/Ψ and $k_F \sim 0.3$ GeV for Ψ'. Finally, in Fig. 8, we show how the wave function of J/Ψ collapses with increasing density.

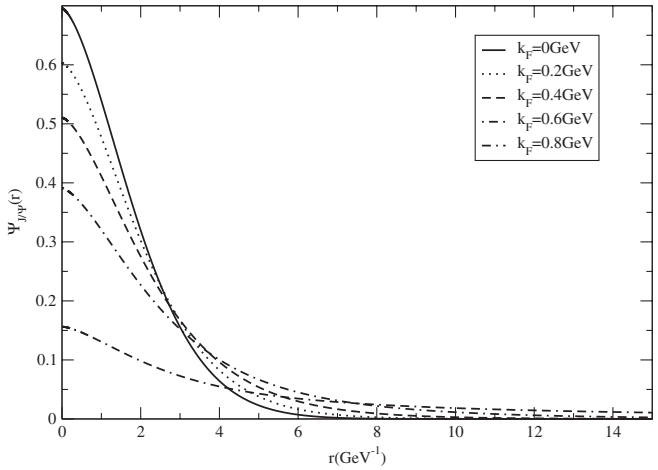

FIG. 8. J/Ψ's wave function $\Psi_{J/\Psi}(r)$ at finite density.

VI. CONCLUSION AND OUTLOOK

In this work we studied the screened quark-quark effective potential at finite temperature and presented a numerical result for the effective potential. We investigated the restoration of chiral symmetry using the many body framework of the Coulomb gauge QCD and find that the transition densities of chiral symmetry restoration and deconfinement need not be related. In the deconfined phase, chiral symmetry can be broken at density $k_F \sim 0.05$ to 0.06 GeV. We also computed the melting density for J/Ψ and Ψ', which we find to be at $k_F \sim 0.9$ GeV and $k_F \sim 0.3$ GeV, respectively. Similar to the situation at high temperature and low density [21,22,43,44], collision of gluons and quarks with heavy quarkonium will reduce the dissociation temperature of quarkonium. We are expecting the same situation occurs at high density and low temperature. As pointed out previously [21,22,43,44], production of quarkonium in heavy-ion collision may provide a clear signal for quark-gluon plasma. Clearly, the collision effect of gluons and quarks with heavy quarkonium should be incorporated in this case, and a detailed discussion of collision dissociation of heavy quarkonium at the phase of high density and low temperature is under way.

[1] J. Adams *et al.* (STAR Collaboration), Nucl. Phys. **A757**, 102 (2005).
[2] D. H. Rischke, Prog. Part. Nucl. Phys. **52**, 197 (2004).
[3] M. Gyulassy and L. McLerran, Nucl. Phys. **A750**, 30 (2005).
[4] J. W. Harris and B. Muller, Annu. Rev. Nucl. Part. Sci. **46**,

71 (1996).
[5] D. J. Gross, R. D. Pisarski, and L. G. Yaffe, Rev. Mod. Phys. **53**, 43 (1981).
[6] J. C. Collins and M. J. Perry, Phys. Rev. Lett. **34**, 1353 (1975).
[7] F. Karsch, Lect. Notes Phys. **583**, 209 (2002).
[8] E. Laermann and O. Philipsen, Annu. Rev. Nucl. Part. Sci. **53**, 163 (2003).
[9] K. Rajagopal, Nucl. Phys. **A642**, c26 (1998).
[10] M. G. Alford, K. Rajagopal, and F. Wilczek, Nucl. Phys. **B537**, 443 (1999).
[11] A. C. Davis and A. M. Matheson, Nucl. Phys. **B246**, 203 (1984).
[12] V. F. Galina and K. S. Viswanathan, Phys. Rev. D **38**, 2000 (1988).
[13] A. Kocic, Phys. Rev. D **33**, 1785 (1986).
[14] L. Y. Glozman and R. F. Wagenbrunn, Phys. Rev. D **77**, 054027 (2008).
[15] L. McLerran and R. D. Pisarski, Nucl. Phys. **A796**, 83 (2007).
[16] Z. Fodor and S. D. Katz, Phys. Lett. B **534**, 87 (2002).
[17] Z. Fodor and S. D. Katz, J. High Energy Phys. 03 (2002) 014.
[18] M. Doring, K. Hubner, O. Kaczmarek, and F. Karsch, Phys. Rev. D **75**, 054504 (2007).
[19] O. Kaczmarek and F. Zantow, Phys. Rev. D **71**, 114510 (2005).
[20] P. Petreczky and K. Petrov, Phys. Rev. D **70**, 054503 (2004).
[21] H. Satz, J. Phys. G **32**, R25 (2006).
[22] C. Y. Wong, Phys. Rev. C **72**, 034906 (2005).
[23] S. Digal, P. Petreczky, and H. Satz, Phys. Lett. B **514**, 57 (2001).
[24] A. Mocsy, P. Petreczky, and J. Casalderrey-Solana, Nucl. Phys. **A783**, 485 (2007); **A785**, 266 (2007).
[25] A. Mocsy and P. Petreczky, Phys. Rev. D **77**, 014501 (2008).
[26] A. P. Szczepaniak and E. S. Swanson, Phys. Rev. D **65**, 025012 (2001).
[27] A. P. Szczepaniak, Phys. Rev. D **69**, 074031 (2004).
[28] N. H. Christ and T. D. Lee, Phys. Rev. D **22**, 939 (1980); Phys. Scr. **23**, 970 (1981).
[29] D. Zwanziger, Nucl. Phys. **B412**, 657 (1994).
[30] V. N. Gribov, Nucl. Phys. **B139**, 1 (1978).
[31] D. Epple, H. Reinhardt, W. Schleifenbaum, and A. P. Szczepaniak, Phys. Rev. D **77**, 085007 (2008).
[32] D. Epple, H. Reinhardt, and W. Schleifenbaum, Phys. Rev. D **75**, 045011 (2007).
[33] H. Reinhardt and C. Feuchter, Phys. Rev. D **71**, 105002 (2005).
[34] C. Feuchter and H. Reinhardt, Phys. Rev. D **70**, 105021 (2004).
[35] A. L. Yaouanc, L. Oliver, O. Pene, J. J. C. Raynal, M. Jarfi, and O. Lazrak, Phys. Rev. D **37**, 3691 (1988).
[36] S. L. Adler and A. C. Davis, Nucl. Phys. **B244**, 469 (1984).
[37] A. Le Yaouanc, L. Oliver, O. Pene, and J. C. Raynal, Phys. Rev. D **29**, 1233 (1984).
[38] P. J. d. Bicudo and J. E. F. Ribeiro, Phys. Rev. D **42**, 1611 (1990).
[39] A. L. Yaouanc, L. Oliver, O. Pene, and J. J. C. Raynal, Phys. Rev. D **29**, 1233 (1984).
[40] A. Le Yaouanc, L. Oliver, O. Pene, J. C. Raynal, M. Jarfi, and O. Lazrak, Phys. Rev. D **39**, 924 (1989).
[41] P. Guo, A. P. Szczepaniak, G. Galata, A. Vassallo, and E. Santopinto, Phys. Rev. D **77**, 056005 (2008).
[42] P. Bicudo, M. Cardoso, P. Santos, and J. Seixas, Phys. Rev. C **72**, 034906 (2005).
[43] M. E. Peskin, Nucl. Phys. **B156**, 365 (1979).
[44] G. Bhanot and M. E. Peskin, Nucl. Phys. **B156**, 391 (1979).